Carcinogenesis vol.33 no.1 pp.184–190, 2012
doi:10.1093/carcin/bgr249
Advance Access publication November 9, 2011

Plumbagin (5-hydroxy-2-methyl-1,4-naphthoquinone), isolated from *Plumbago zeylanica*, inhibits ultraviolet radiation-induced development of squamous cell carcinomas

Jordan M.Sand[1], Bilal Bin Hafeez[2], Mohammad Sarwar Jamal[2], Olya Witkowsky[2], Emily M.Siebers[2], Joseph Fischer[2] and Ajit K.Verma[2,*]

[1]Molecular and Environmental Toxicology and [2]Department of Human Oncology, School of Medicine and Public Health, Wisconsin Institutes of Medical Research, 1111 Highland Avenue, University of Wisconsin–Madison, Madison, WI 53705, USA

*To whom correspondence should be addressed. Tel: +1 608 263 9136; Fax: +1 608 262 6654;
Email: akverma@facstaff.wisc.edu

Plumbagin (PL) (5-hydroxy-2-methyl-1,4-napthoquinone), a medicinal plant-derived naphthoquinone, was isolated from the roots of the *Plumbago zeylanica* L. (also known as Chitrak). The roots of *P. zeylanica* L. have been used in Indian medicine for >2500 years as an anti-atherogenic, cardiotonic, hepatoprotective and neuroprotective agent. We present here that topical application of non-toxic doses (100–500 nmol) of PL to skin elicits dose-dependent inhibition of ultraviolet radiation (UVR)-induced development of squamous cell carcinomas (SCC). In this experiment, FVB/N mice were exposed to UVR (2 kJ/m^2) three times weekly from a bank of six Kodacel-filtered FS40 sunlamps (∼60% UVB and 40% UVA). Carcinoma incidence in mice treated with vehicle, 100, 200 or 500 nmol PL, at 44 weeks post-UVR, were 86, 80 ($P = 0.67$), 53 ($P = 0.12$) and 7% ($P = 0.0075$), respectively. Both vehicle and PL-treated mice gained weight and did not exhibit any signs of toxicity during the entire period of the experiment. Molecular mechanisms associated with inhibition of UVR-induced development of SCC involved induction of apoptosis and inhibition of cell proliferation. Specific findings are that PL treatment (i) inhibited UVR-induced DNA binding of activating protein-1, nuclear factor-kappaB, Stat3 transcription factors and Stat3-regulated molecules (cdc25A and Survivin); (ii) inhibited protein levels of pERK1/2, PI3K85, pAKTSer473, Bcl$_2$, BclxL, proliferating cell nuclear antigen and cell cycle inhibitory proteins p27 and p21 and (iii) increased UVR-induced Fas-associated death domain expression, poly (ADP-ribose) polymerase protein cleavage and Bax/Bcl$_2$ ratio. Taken together, our findings suggest that PL may be a novel agent for the prevention of skin cancer.

Introduction

Skin cancer is the most common malignancy encountered in USA with an expected diagnosis of 1.3 million new cases of non-melanoma skin cancer each year (1). Squamous cell carcinoma (SCC) and basal cell carcinoma (BCC) are the most common non-melanoma forms of human skin cancer (2–4). BCC is rarely life threatening because it is slow growing and mostly localized (3). SCC, unlike BCC, invades the nearby tissues. The first site of metastasis is usually a regional lymph node before metastatic growth in distant sites such as the lungs and brain. Although mortality due to SCC and BCC is low, it still poses a significant societal risk (3). The most important risk factor for non-melanoma skin cancer is chronic exposure to ultraviolet radiation (UVR) in sunlight (5,6). The UV spectrum, part of the electromagnetic spectrum, lies between visible light and X-rays and is divided conventionally into three categories: UVA (315–400 nm), UVB (280–315 nm) and UVC (190–280 nm). UVA and UVB components of sunlight are the most prominent and ubiquitous carcinogenic wavelengths in our natural environment (7). We found that plumbagin (PL), a medicinal plant-derived naphthoquinone, inhibits UVR-induced development of SCC.

PL is a quinoid constituent isolated from the roots of the medicinal plant *Plumbago zeylanica* L. (also known as Chitrak). PL has also been found in *Juglans regia* (English walnut), *Juglans cinerea* (butternut and white walnut) and *Juglans nigra* (black walnut) (8). PL has been shown to exert anticancer and antiproliferative activities in animal models and in cell culture (8). PL fed in the diet (200 ppm) inhibits azoxymethane-induced intestinal tumors in rats (9). PL inhibits ectopic growth of breast cancer MDA-MB-231 cells (10), non-small cell lung cancer A549 cells (11) and melanoma A375-S2 cells in athymic nude mice (12). PL also inhibits the growth of human prostate cancer (PCa) cell lines *in vitro* (13). We have shown that PL inhibits prostate cancer growth *in vitro* and *in vivo* (14). PL has been shown to exert antibacterial, antifungal, anti-atherosclerotic and anticancer effects (8) through a variety of mechanisms, including induction of reactive oxygen species (12); suppression of nuclear factor-kappaB (NF-κB) (8), AKT/mTOR (10) and Stat3 (15); induction of p53 and c-jun N-terminal kinase (11), activation of the NRF2-ARE pathway (16) and inhibition of histone acetyltransferase p300 (17) and VEGFR2-mediated Ras signaling pathway (18). We present in this communication for the first time that topical treatment of PL inhibits UVR-induced development of SCC in mice. PL-caused inhibition of UVR-induced development of SCC accompanied modulation of molecular components of cell proliferation and apoptosis.

Abbreviations: BCC, basal cell carcinoma; EDTA, ethylenediaminetetraacetic acid; FADD, Fas-associated death domain; HEPES, *N*-2-hydroxyethylpiperazine-*N*′-2-ethanesulfonic acid; NF-κB, nuclear factor-kappaB; PL, plumbagin; SCC, squamous cell carcinoma; UVR, ultraviolet radiation.

Materials and methods

Chemicals, antibodies and assay kits

Antibodies to actin, Stat3, Fas-associated death domain (FADD), PI3K85, pMEK1/2, pERK1/2, MEK1/2, ERK1/2, p21, p27, Bcl2, BclxL and Bax were purchased from Santa Cruz Biotechnologies (Santa Cruz, CA). Antibodies to poly (ADP-ribose) polymerase protein/cleaved poly (ADP-ribose) polymerase protein were purchased from Enzo Life Sciences (Plymouth Meeting, PA). Antibodies to pStat3Ser727 and pStat3Tyr705 were from BD Biosciences (San Jose, CA) and to pAKTSer473 and AKT were from Cell Signaling (Danvers, MA). Anti-mouse, anti-goat and anti-rabbit secondary antibodies were purchased from Thermo Scientific (Rockford, IL). The oligonucleotides for activating protein-1 (AP-1) (5′-CGCTTGATGACTCAGCCGGAA-3′), NF-κB (5′-AGTTGAGGGGACTTTCCCAGGC-3′) and Stat3 (5′-GATCCTTCTGGGAATTCCTAG ATC-3′) were obtained from Santa Cruz Biotechnology. PL (practical grade, purity >95%, molecular weight: 188.18) was purchased from Sigma–Aldrich.

Mice and UVR treatment

The UVR source was a bank of six Kodacel-filtered FS-40 sunlamps (∼60% UVB and 40% UVA). Female FVB/N mice were purchased from Taconic (Pharmington, NY). The dorsal skin of the mice (8 weeks old) was shaved 3–4 days before experimentation. UVR dose was routinely measured using a UVX radiometer. Mice were exposed to UVR as indicated in each experiment. Stock solution (20 mM) of PL was prepared in dimethyl sulfoxide and further diluted in acetone to obtain desired dose for topical application.

Electrophoretic mobility shift assay

Mice were shaved and depilated before experimentation. Mice were exposed to UVR once and then 15 min post-UVR, treated with either vehicle or 500 nmol PL. Mice were killed 1, 2 and 3 h post-UVR. Mouse skin was excised and scraped to remove subcutaneous fat. The epidermis was scraped off on an ice-cold glass plate and nuclear protein extracts were prepared by lysing scraped epidermis in a hypotonic solution [10 mmol/l *N*-2-hydroxyethylpiperazine-*N*′-2-ethanesulfonic acid (HEPES, pH 7.5), 10 mmol/l KCl, 0.1 mmol/l ethylenediaminetetraacetic acid (EDTA, pH 8.0), 0.1 mmol/l

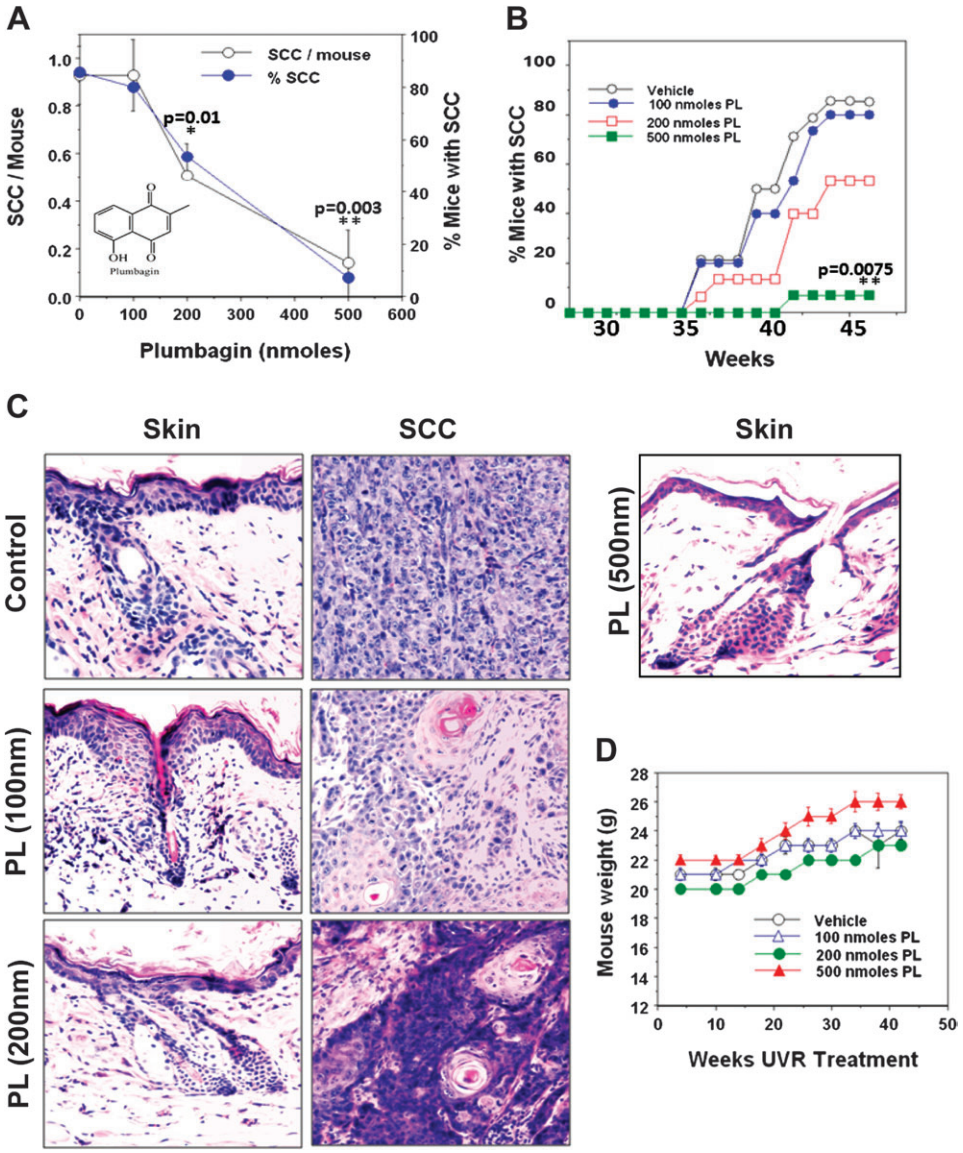

Fig. 1. PL treatment inhibits UVR-induced development of SCC. Female FVB/N mice, at 8 weeks of age, were shaved 3 days before the start of UVR exposure and then were exposed to UVR (2 kJ/m^2) three times weekly from a bank of six Kodacel-filtered FS40 sunlamps. There were 14 mice per group. Carcinomas were recorded as downward invading lesions, which were confirmed histologically. The carcinoma data are expressed as a percentage of the effectual total. Carcinoma incidence was analyzed using Cox proportional hazards model. **(A)** Comparison of carcinoma multiplicity and SCC incidence at 42 weeks. **(B)** Percentage of SCC incidence in vehicle and PL-treated mice at various weeks post-UVR exposure. *P* values are shown in figures (A and B) comparing vehicle and PL-treated mice. **(C)** Hematoxylin and eosin staining of uninvolved skin and SCC from vehicle and PL-treated animals. **(D)** Mouse body weight of vehicle and PL-treated animals at various weeks post-UVR exposure.

ethyleneglycol-bis(aminoethylether)-tetraacetic acid (pH 8.0), 1 mmol/l dithiothreitol, 0.5 mmol/l phenylmethylsulfonyl fluoride, 0.5 mg/ml benzamide, 2 μg/ml aprotinin and 2 μg/ml leupeptin], with detergent [Nonidet P-40 at 6.25% (vol/vol)] followed by low-speed (1500*g* for 30 s) centrifugation to collect nuclei. Nuclear proteins were extracted in a high-salt buffer [20 mmol/l HEPES (pH 7.5), 0.4 mol/l NaCl, 1 mmol/l EDTA (pH 8.0), 1 mmol/l ethyleneglycol-bis (aminoethylether)-tetraacetic acid (pH 8.0), 1 mmol/l dithiothreitol, 1 mmol/l phenylmethylsulfonyl fluoride, 0.5 mg/ml benzamide, 2 μg/ml aprotinin and 2 μg/ml leupeptin] incubated on ice for 15 min and then nuclear membranes and genomic DNA were removed by high-speed (16 000*g*) centrifugation for 5 min. Nuclear protein extracts were stored at −70°C until used. Nuclear protein extracts were incubated in a final volume of 20 μl of 10 mmol/l HEPES (pH 7.9), 80 mmol/l NaCl, 10% glycerol, 1 mmol/l dithiothreitol, 1 mmol/l EDTA and 100 μg/ml poly(deoxyinosinic-deoxycytidylic acid) for 15 min. ^{32}P-radiolabeled double-stranded oligonucleotides consisting of the consensus binding sequences of AP-1, NF-κB or Stat3 were then added and the complexes were incubated for 20 min at room temperature. The protein–DNA complexes were resolved on a 4.5% acrylamide gel containing 2.5% glycerol in 0.5× Tris–borate–EDTA at room temperature. Gels were dried and autoradiographed to determine binding activity (16).

Western blot analysis

Mice were shaved before experimentation. At appropriate times, as indicated in each experiment, after UVR exposure, mouse skin was excised and scraped to remove subcutaneous fat. The epidermis was scraped off on an ice-cold glass plate and homogenized in lysis buffer [50 mmol/l HEPES, 150 mmol/l NaCl, 10% glycerol, 1% Triton X-100, 1.5 mmol/l $MgCl_2$, 10 μg/ml aprotinin, 10 μg/ml leupeptin, 1 mmol/l phenylmethylsulfonyl fluoride, 200 μmol/l Na_3VO_4, 200 μmol/l NaF and 1 mmol/l ethyleneglycol-bis(aminoethylether)-tetraacetic acid (final pH 7.5)]. The homogenate was rotated for 30 min at 4°C to aid in lysing and centrifuged at 14 000*g* for 30 min at 4°C. Epidermal cell lysates (25 μg protein) were fractionated on 10–15% Criterion precast sodium dodecyl sulfate–polyacrylamide gels (Bio-Rad Laboratories, Hercules, CA). The fractionated proteins were transferred to 0.45 μm Hybond-P polyvinylidene difluoride transfer membrane (Amersham Life Sciences, Piscataway, NJ). The membrane was then incubated with the specific antibody followed by the

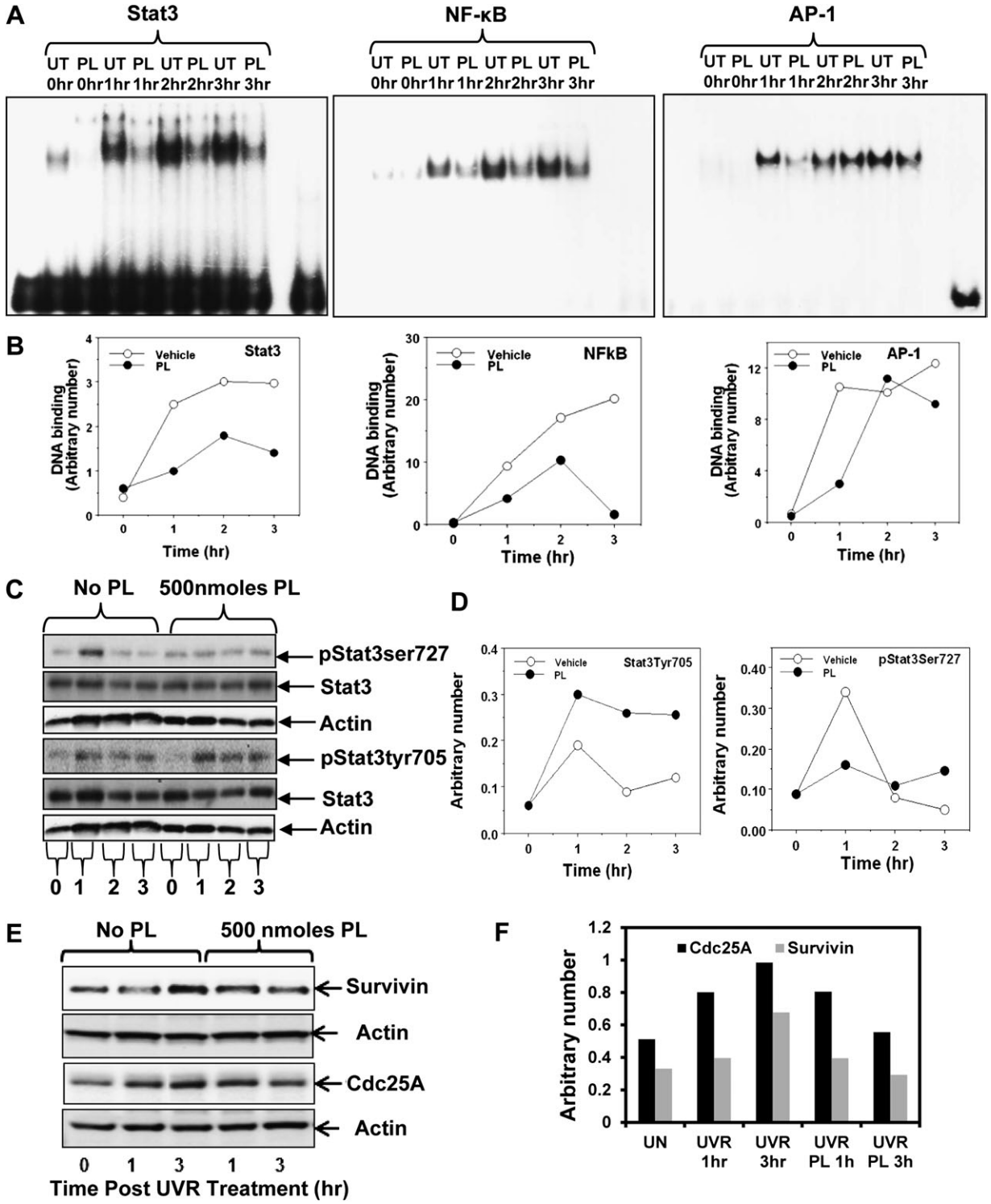

Fig. 2. PL treatment inhibits Stat3, NF-κB and AP-1 DNA binding and expression of phosphorylated Stat3Ser727. Female FVB/N mice were shaved 48 h before experimentation. Mice were exposed to a single dose of 2 kJ/m^2 UVR and then treated with either vehicle (acetone) or 500 nmol of PL and killed 1, 2 and 3 h post-UVR exposure. Skin was excised and epidermal nuclear lysates and whole epidermal tissue lysates were prepared for Electrophoretic mobility shift assay and western blot analysis, respectively. **(A)** DNA-binding activity of Stat3, NF-κB and AP-1 by Electrophoretic mobility shift assay. **(B)** Quantitation of DNA-binding activity of Stat3, NF-κB and AP-1. **(C)** Protein levels of pStat3Ser727, pStat3Tyr705 and total Stat3 in mouse epidermis obtained from vehicle and PL-treated animals after UVR treatments as determined by western blot analysis. Equal loading of protein was confirmed by stripping and re-probing the blots with actin antibody. **(D)** Quantitation of the western blots for pStat3Ser727 and pStat3Tyr705 are shown in (C). Arbitrary numbers shown in graph are normalized to actin. **(E)** Protein levels of survivin and cdc25A in vehicle and PL-treated mouse epidermis tissues as determined by western blot analysis. **(F)** Quantitation of survivin and cdc25A.

appropriate horseradish peroxidase-conjugated secondary antibody (Thermo Scientific). The detection signal was developed with Amersham's enhanced chemiluminescence reagent and images were captured by using FOTO/Analyst Luminary Work Station (Fotodyne). The western blot results were quantitated by densitometric analysis using Total lab Nonlinear Dynamic Image analysis software (Nonlinear USA, Durham, NC).

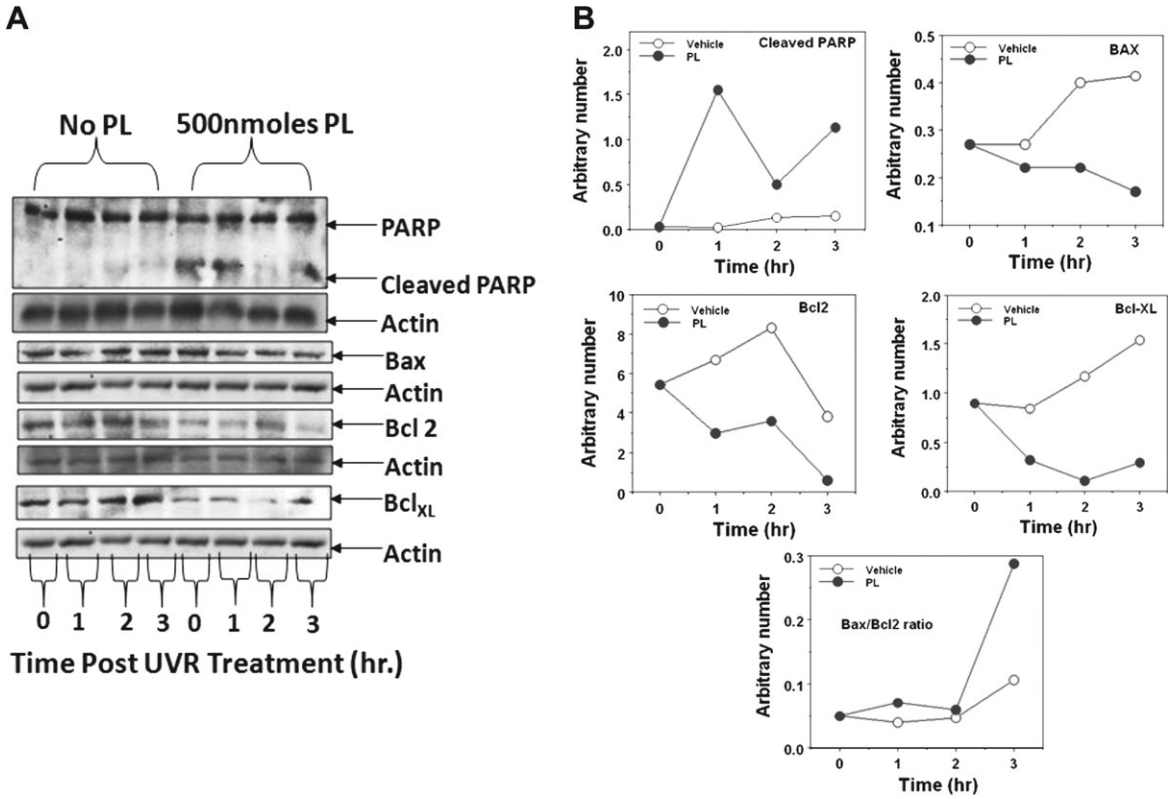

Fig. 3. PL treatment modulates UVR-induced apoptotic proteins [poly (ADP-ribose) polymerase protein, Bax, Bcl2 and Bcl-xL]. Female FVB/N mice were shaved 48 h before experimentation. Mice are exposed to a single dose of 2 kJ/m^2 UVR and then treated with either vehicle or PL. Mice were killed 1, 2 and 3 h post-UVR exposure. **(A)** The epidermal lysate (25 μg protein) was subjected for western blot analysis for indicated proteins. Equal loading of protein was confirmed by stripping and re-probing the blots with actin antibody. **(B)** Quantitation of the western blots of indicated proteins in (A).

Statistical methods

The primary end point of interest was early death or carcinoma. Those mice that did not reach the end point or develop carcinoma were censored at the last point that data were available for them. A Cox proportional hazards model was created, modeling the end point on treatment group as a categorical variable. A Cox proportional hazards model is a widely used method of survival analysis, which relates time to event to one or more covariates. As the overall model was significant, P values for comparisons between each treatment group and the acetone group were adjusted using Hochberg's step-up method. To further explore the dose–response relationship, Cox proportional hazards models using modeling dose as a continuous variable were examined. The data analysis for this paper was generated using SAS software, Version 9.1, of the SAS System for Unix, Copyright© 2002–2003, SAS Institute. SAS and all other SAS Institute products or service names are registered trademarks or trademarks of SAS Institute , Cary, NC.

Results

PL inhibits UVR-induced development of SCC

The effects of PL on UVR-induced development of SCC in FVB/N mice were determined. The selective advantage of FVB/N model is that these mice, as opposed to SKH-1 hairless mice, bypass the stage of papillomas and only develop SCC. The main goal of this study was to determine the effect of PL on UVR-induced development of SCC. In this experiment (Figure 1), mice were exposed to UVR (2 kJ/m^2) three times a week (Monday, Wednesday and Friday). PL was applied at 15 min after each UVR exposure. PL at various doses (100, 200 or 500 nmol) was applied topically to skin in 0.2 ml acetone. A dose-dependent inhibition of both SCC multiplicity and incidence was observed (Figure 1A). Carcinoma multiplicity was as follows: (vehicle, 0.93), (100 nmol PL, 0.93), (200 nmol PL, 0.4) and (500 nmol PL, 0.14). The carcinoma multiplicity in both 200 and 500 nmol PL-treated groups was found to be statistically significant from the control ($^*P = 0.01$, $^{**}P = 0.003$) (Figure 1A). At week 44, 85% of untreated mice had carcinomas, whereas the carcinoma incidence in 100, 200 and 500 nmol PL-treated groups was 80 ($P = 0.67$), 53 ($P = 0.12$) and 7% ($P = 0.0075$), respectively (Figure 1B). All UVR-induced skin tumors were diagnosed histologically as moderately differentiated SCC (Figure 1C). It appears from the hematoxylin and eosin-stained sections of uninvolved skin that PL inhibited UVR-induced hyperplasia (Figure 1C). Both vehicle and PL-treated mice gained weight and did not exhibit any signs of toxicity during the entire period of the experiment (Figure 1D).

PL inhibits UVR-induced DNA binding of Stat3, NF-κB and AP-1 transcription factors

UVR mediates activation of transcription factors Stat3, NF-κB and AP-1, which culminates in the expression of both survival and apoptotic genes (5,8,19,20). A possibility was explored that PL inhibition of SCC development may involve inhibition of UVR-induced DNA binding of Stat3, NF-κB and AP-1. In this experiment (Figure 2), FVB/N mice were treated once with UVR (2 kJ/m^2) and then 15 min later either vehicle (acetone) or 500 nmol PL applied topically. Mice were killed 1, 2 and 3 h post-UVR treatment. Skin was excised and both nuclear protein extracts and total epidermal lysates were prepared. The nuclear protein extracts were analyzed by Electrophoretic mobility shift assay. The total epidermal lysates were used to determine expression of indicated proteins by western blot analyses. PL treatment inhibited UVR-induced DNA binding of Stat3, NF-κB and AP-1 (Figure 2A and B). As shown in Figure 2C and D, PL treatment inhibited Stat3Ser727 phosphorylation. However, PL treatment did not inhibit Stat3Tyr705 phosphorylation. Also, PL inhibited UVR-mediated Stat3-regulated gene expression (survivin, cdc25A) (Figure 2E and F).

PL modulates the UVR-induced apoptotic proteins

As shown in Figure 3, PL treatment enhanced the expression of cleaved poly (ADP-ribose) polymerase protein, which is considered

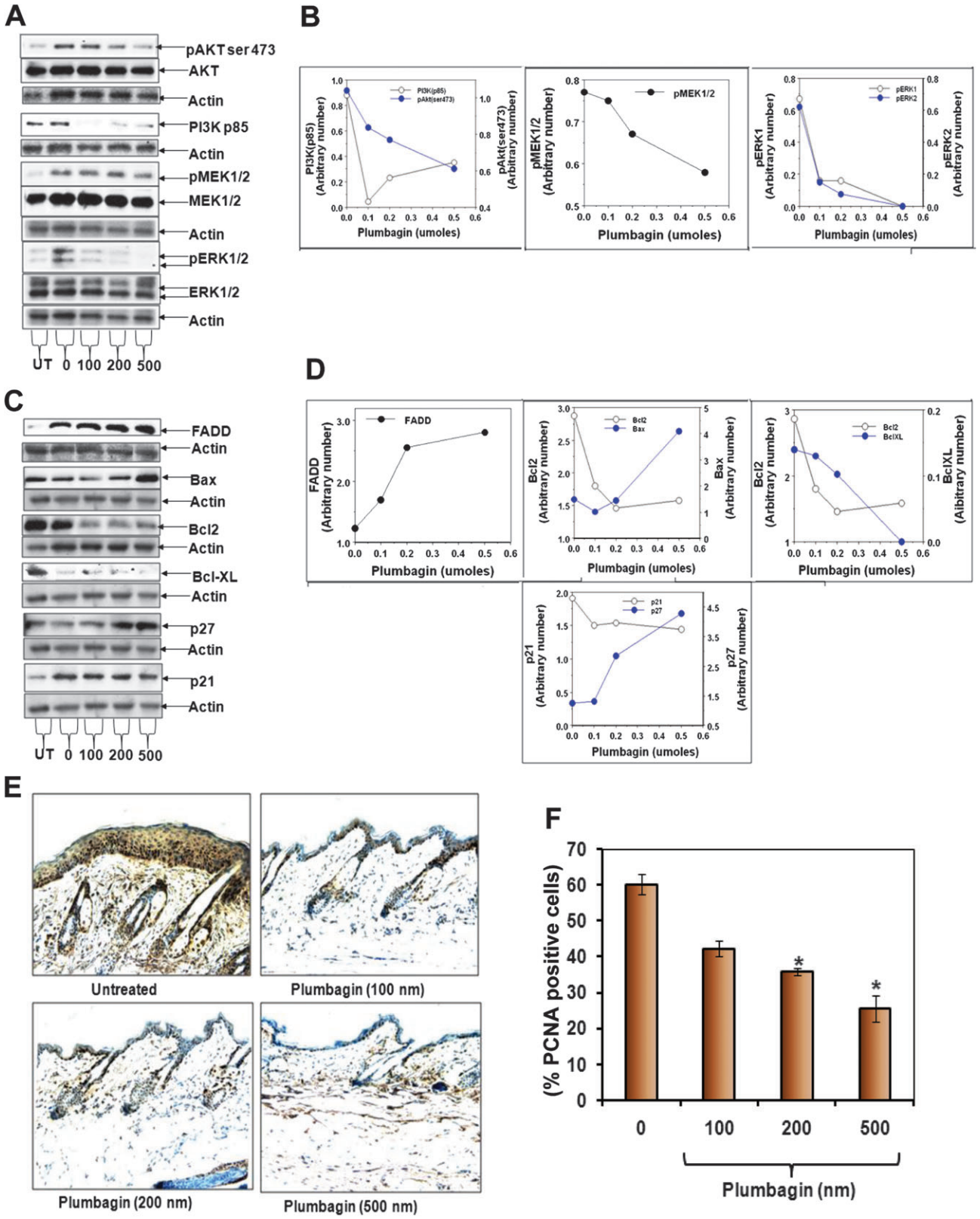

Fig. 4. Effects of PL on chronic UVR-induced expression of pro-apoptotic and pro-survival proteins. Female FVB/N mice were shaved 48 h before experiment. Mice were exposed to 2 kJ/m^2 UVR thrice weekly. Vehicle (acetone) or PL was applied 15 min after each UVR treatment for 4 weeks. Mice were killed 6 h after final UVR exposure. The epidermal lysates were prepared and 25 μg proteins were subjected for western blot analysis. Equal loading was confirmed by stripping and re-probing the blots with actin antibody. **(A)** Dose-dependent effect of PL on protein levels of pAKTSer473, PI3K85, pMEK1/2, MEK1/2, pERK1/2 and ERK1/2. **(B)** Quantitation of indicated blots shown in (A). **(C)** Dose-dependent effect of PL on protein levels of FADD, Bax, Bcl2, Bcl-xL, p27 and p21. **(D)** Quantitation of indicated blots shown in (C). **(E)** Representative pictures of immunohistochemistry of proliferating cell nuclear antigen (PCNA) in mouse skin obtained from vehicle and PL-treated animals. **(F)** Bar graph illustrating percentage of PCNA-positive cells in mouse epidermis of vehicle and PL-treated animals. Each value is the percent mean ± standard error of the mean of PCNA-positive cells counted from 10 random areas from each mouse skin.

a marker of apoptosis (Figure 3A and B). PL treatment showed a marked decrease in BclxL protein levels (Figure 3A and B). PL treatment also resulted in an increase in the Bax/Bcl_2 ratio (Figure 3A and B) implying induction of apoptosis.

PL treatment inhibits components of the cell survival pathways and increases proapoptotic signals

AKT, PI3K, MEK1/2 and ERK1/2 are major components of cell survival pathways. We determined whether PL treatment inhibits UVR-induced activation of these survival pathways. In this experiment (Figure 4), mice were exposed to UVR (2 kJ/m^2 thrice weekly) for 4 weeks. Mice were treated with various doses (0, 100, 200 and 500 nmol) of PL 15 min after each UVR treatment. Mice were killed at 6 h after last UVR treatment. Skin was excised and total epidermal lysates were prepared to determine the expression of indicated proteins by western blot analysis. PL treatment inhibited the expression of phosphorylated AKT (ser473), PI3K85 (regulatory subunit), MEK1/2 and ERK1/2 (Figure 4A and B). FADD is an adapter protein, which associates with death receptors (Fas and TNFRI) and transmits apoptotic signals from outside the cell to the downstream initiator caspase-8. Also, FADD is connected to the mitochondrial intrinsic apoptotic signal transduction pathway. In the same experiment (Figure 4C and D), PL treatment increased UVR-induced expression of FADD protein and Bax while decreasing the expression of pro-survival proteins Bcl2 and BclxL. PL treatment induced the expression of cell cycle inhibitory proteins p21 and p27 (Figure 4C and D). As shown in Figure 4E and F, PL treatment inhibited UVR-induced expression of proliferating cell nuclear antigen-positive cells.

Discussion

We present that PL, a medicinal plant-derived napthoquinone, prevents UVR-induced development of mouse SCC (Figure 1). PL, at a 500 nmol dose, almost completely inhibited SCC development. Since PL was applied post-UVR treatment, inhibitory effects of PL cannot be attributable to a sunscreen property.

PL has also been extensively evaluated for toxic side effects in rodents. Side effects included diarrhea, skin rashes, hepatic (21) and reproductive toxicity (22). The LD50 for these side effects depends upon the administration method. In mice, it was 8–65 mg/kg body weight for oral administration and 16 mg/kg body weight for intraperitoneal administration. These toxic side effects are dose related and it is noteworthy that they are not observed at doses (2 mg/kg body weight intraperitoneally or 200 ppm in diet) reported to elicit chemopreventive (ref. 14) and therapeutic effects. In our findings (Figure 1), mice exhibited no signs of toxicity (e.g. skin rashes, diarrhea or hepatic toxicity) at any of the doses (100, 200 and 500 nmol). Mice gained weight (Figure 1D). These results indicate that non-toxic doses of PL can prevent UVR-induced development of SCC.

PL treatment indiscriminately inhibited DNA binding of Stat3, NF-κB and AP-1, implying inhibition of these transcription factor-regulated genes are involved in SCC prevention. Sandur *et al.* (8) have reported that PL disrupts cell proliferation, carcinogenesis and radioresistance. The mechanism by which PL inhibits carcinogenesis may be due to inhibition of DNA binding of NF-κB. We observed that PL not only inhibited NF-κB DNA binding but also DNA binding of Stat3 and AP-1 (Figure 2A and B). Stat3 has two conserved amino acid residues (Ser727 and Tyr705) that are phosphorylated during Stat3 activation. The transcriptional activity of Stat3 involves the dimerization, nuclear translocation, DNA binding and recruitment of transcriptional co-activators (23). Phosphorylation of the tyrosine residue is mediated by many varied polypeptides and has been shown to be essential for the STAT homo- or heterodimerzation and nuclear translocation (24). Evidence indicates that the phosphorylation of both residues (Ser727 and Tyr 705) is necessary for complete activation of Stat3 (25). We have reported that PKCϵ interacts with Stat3 and phosphorylates Stat3Ser727 (26).

PL inhibits the activation of PI3K/AKT, MEK1/2 and ERK1/2, which are major components of the cell survival pathway (Figure 4A and B). The mechanism by which PL suppresses the activation of AP-1, NF-κB and Stat3 in epidermal cells is unclear. However, PL inhibits expression of PI3K/AKT, MEK1/2 and ERK1/2, which may play a role in the activation of AP-1, NF-κB and Stat3.

PL treatment was also found to increase apoptotic markers such as Bax/Bcl2 ratio and FADD expression. There was also a decrease in pro-survival proteins Bcl2 and BclxL. These results indicate that PL-caused inhibition of SCC induction may involve induction of cell death. The results involving the induction of apoptosis by PL are consistent with findings using cancer cell lines such as ovarian cancer BG1 (27), cervical cancer cells (28) and breast cancer cells (29). PL-induced apoptosis involves G_2–M arrest and generation of reactive oxygen species (28). Reactive oxygen species-mediated inhibition of topoisomerase II has been suggested to be a mechanism contributing to the apoptosis-inducing properties of PL (30).

Chemoprevention by topical application of natural products has been demonstrated with many different agents. These agents were found to be limited in their effectiveness. Epigallocatechin gallate applied at 1 mg/cm^2 caused a 60% decrease in tumor incidence (31). Resveratrol applied topically at 50 μM/200 μl after UVR exposure decreased tumorogenesis by nearly 40% (32). Silymarin applied topically at 9 mg/200 μl to SKH-1 hairless mice decreased tumor incidence by 20% (33). Here we report that PL inhibits tumor incidence by 79% at 0.5 μmoles dose. PL is 20% more effective at chemoprevention than the next best topically applied natural agent.

In summary, PL, a naturally occurring naphthoquinone (8,34), inhibits UVR-induced development of SCC in mouse skin. PL-induced inhibition of SCC accompanies inhibition of multiple targets including transcription factors AP-1, NF-κB and Stat3. Taken together, our results indicate that PL could be explored for the prevention of UVR-induced skin cancer.

Funding

National Institutes of Health (CA35368) to A.K.V.; Molecular and Environmental Toxicology Center pre-doctoral training grant (T32ES007015) to J.M.S.

Acknowledgements

We are also thankful to Nancy E. Dreckschmidt for her technical support in Electrophoretic mobility shift assay experiments.

Conflict of Interest Statement: None declared.

References

1. Jemal,A. *et al*. (2009) Cancer statistics, 2009. *CA Cancer J. Clin.*, **59**, 225–249.
2. Armstrong,B.K. *et al*. (2001) The epidemiology of UV induced skin cancer. *J. Photochem. Photobiol. B*, **63**, 8–18.
3. de Gruijl,F.R. (2002) Photocarcinogenesis: UVA vs. UVB radiation. *Skin Pharmacol. Appl. Skin Physiol.*, **15**, 316–320.
4. Nguyen,T.H. *et al*. (2002) Nonmelanoma skin cancer. *Curr. Treat. Options Oncol.*, **3**, 193–203.
5. Cooper,S.J. *et al*. (2007) Ultraviolet B regulation of transcription factor families: roles of nuclear factor-kappa B (NF-kappaB) and activator protein-1 (AP-1) in UVB-induced skin carcinogenesis. *Curr. Cancer Drug Targets*, **7**, 325–334.
6. Molho-Pessach,V. *et al*. (2007) Ultraviolet radiation and cutaneous carcinogenesis. *Curr. Probl. Dermatol.*, **35**, 14–27.
7. Wheeler,D.L. *et al*. (2004) Protein kinase C epsilon is an endogenous photosensitizer that enhances ultraviolet radiation-induced cutaneous damage and development of squamous cell carcinomas. *Cancer Res.*, **64**, 7756–7765.
8. Sandur,S.K. *et al*. (2006) Plumbagin (5-hydroxy-2-methyl-1,4-naphthoquinone) suppresses NF-kappaB activation and NF-kappaB-regulated gene products through modulation of p65 and IkappaBalpha kinase activation, leading to potentiation of apoptosis induced by cytokine and chemotherapeutic agents. *J. Biol. Chem.*, **281**, 17023–17033.

9. Sugie,S. *et al*. (1998) Inhibitory effects of plumbagin and juglone on azoxymethane-induced intestinal carcinogenesis in rats. *Cancer Lett.*, **127**, 177–183.
10. Kuo,P.L. *et al*. (2006) Plumbagin induces G2-M arrest and autophagy by inhibiting the AKT/mammalian target of rapamycin pathway in breast cancer cells. *Mol. Cancer Ther.*, **5**, 3209–3221.
11. Hsu,Y.L. *et al*. (2006) Plumbagin (5-hydroxy-2-methyl-1,4-naphthoquinone) induces apoptosis and cell cycle arrest in A549 cells through p53 accumulation via c-Jun NH2-terminal kinase-mediated phosphorylation at serine 15 *in vitro* and *in vivo*. *J. Pharmacol. Exp. Ther.*, **318**, 484–494.
12. Wang,C.C. *et al*. (2008) Plumbagin induces cell cycle arrest and apoptosis through reactive oxygen species/c-Jun N-terminal kinase pathways in human melanoma A375.S2 cells. *Cancer Lett.*, **259**, 82–98.
13. Powolny,A.A. *et al*. (2008) Plumbagin-induced apoptosis in human prostate cancer cells is associated with modulation of cellular redox status and generation of reactive oxygen species. *Pharm. Res.*, **25**, 2171–2180.
14. Aziz,M.H. *et al*. (2008) Plumbagin, a medicinal plant-derived naphthoquinone, is a novel inhibitor of the growth and invasion of hormone-refractory prostate cancer. *Cancer Res.*, **68**, 9024–9032.
15. Sandur,S.K. *et al*. (2010) 5-Hydroxy-2-methyl-1,4-naphthoquinone, a vitamin K3 analogue, suppresses STAT3 activation pathway through induction of protein tyrosine phosphatase, SHP-1: potential role in chemosensitization. *Mol. Cancer Res.*, **8**, 107–118.
16. Son,T.G. *et al*. (2010) Plumbagin, a novel Nrf2/ARE activator, protects against cerebral ischemia. *J. Neurochem.*, **112**, 1316–1326.
17. Ravindra,K.C. *et al*. (2009) Inhibition of lysine acetyltransferase KAT3B/p300 activity by a naturally occurring hydroxynaphthoquinone, plumbagin. *J. Biol. Chem.*, **284**, 24453–24464.
18. Lai,L. *et al*. (2011) Plumbagin inhibits tumor angiogenesis and tumor growth through VEGFR2-mediated Ras signaling pathway. *Br. J. Pharmacol.* doi: 10.1111/j.1476-5381.2011.01532.x.[Epub ahead of print].
19. Aziz,M.H. *et al*. (2007) Protein kinase Cepsilon interacts with signal transducers and activators of transcription 3 (Stat3), phosphorylates Stat3Ser727, and regulates its constitutive activation in prostate cancer. *Cancer Res.*, **67**, 8828–8838.
20. Sano,S. *et al*. (2008) Impact of Stat3 activation upon skin biology: a dichotomy of its role between homeostasis and diseases. *J. Dermatol. Sci.*, **50**, 1–14.
21. Parimala,R. *et al*. (1993) Effect of plumbagin on some glucose metabolising enzymes studied in rats in experimental hepatoma. *Mol. Cell Biochem.*, **125**, 59–63.
22. Azad Chowdhury,A.K. *et al*. (1982) Antifertility activity of *Plumbago zeylanica* Linn. root. *Indian J. Med. Res.*, **76** (suppl.), 99–101.
23. Li,L. *et al*. (2004) A STAT3 dimer formed by inter-chain disulphide bridging during oxidative stress. *Biochem. Biophys. Res. Commun.*, **322**, 1005–1011.
24. Chan,K.S. *et al*. (2004) Epidermal growth factor receptor-mediated activation of Stat3 during multistage skin carcinogenesis. *Cancer Res.*, **64**, 2382–2389.
25. Akira,S. (2000) Roles of STAT3 defined by tissue-specific gene targeting. *Oncogene*, **19**, 2607–2611.
26. Aziz,M.H. *et al*. (2007) Protein kinase C epsilon, which sensitizes skin to sun's UV radiation-induced cutaneous damage and development of squamous cell carcinomas, associates with Stat3. *Cancer Res.*, **67**, 1385–1394.
27. Thasni,K.A. *et al*. (2008) Estrogen-dependent cell signaling and apoptosis in BRCA1-blocked BG1 ovarian cancer cells in response to plumbagin and other chemotherapeutic agents. *Ann. Oncol.*, **19**, 696–705.
28. Srinivas,P. *et al*. (2004) Plumbagin induces reactive oxygen species, which mediate apoptosis in human cervical cancer cells. *Mol. Carcinog.*, **40**, 201–211.
29. Ahmad,A. *et al*. (2008) Plumbagin-induced apoptosis of human breast cancer cells is mediated by inactivation of NF-kappaB and Bcl-2. *J. Cell Biochem.*, **105**, 1461–1471.
30. Kawiak,A. *et al*. (2007) Induction of apoptosis by plumbagin through reactive oxygen species-mediated inhibition of topoisomerase II. *Toxicol. Appl. Pharmacol.*, **223**, 267–276.
31. Mantena,S.K. *et al*. (2005) Epigallocatechin-3-gallate inhibits photocarcinogenesis through inhibition of angiogenic factors and activation of CD8+ T cells in tumors. *Photochem. Photobiol.*, **81**, 1174–1179.
32. Aziz,M.H. *et al*. (2005) Chemoprevention of skin cancer by grape constituent resveratrol: relevance to human disease? *FASEB J.*, **19**, 1193–1195.
33. Mallikarjuna,G. *et al*. (2004) Silibinin protects against photocarcinogenesis via modulation of cell cycle regulators, mitogen-activated protein kinases, and Akt signaling. *Cancer Res.*, **64**, 6349–6356.
34. Padhye,S. *et al*. (2010) Perspectives on medicinal properties of plumbagin and its analogs. *Med. Res. Rev.*, **9.** [Epub ahead of print].

Received July 25, 2011; revised October 5, 2011; accepted October 29, 2011